How natural and anthropogenic influences alter global and regional surface temperatures: 1889 to 2006

Judith L. Lean[1] and David H. Rind[2]

Received 2 June 2008; revised 1 August 2008; accepted 8 August 2008; published 16 September 2008.

[1] To distinguish between simultaneous natural and anthropogenic impacts on surface temperature, regionally as well as globally, we perform a robust multivariate analysis using the best available estimates of each together with the observed surface temperature record from 1889 to 2006. The results enable us to compare, for the first time from observations, the geographical distributions of responses to individual influences consistent with their global impacts. We find a response to solar forcing quite different from that reported in several papers published recently in this journal, and zonally averaged responses to both natural and anthropogenic forcings that differ distinctly from those indicated by the Intergovernmental Panel on Climate Change, whose conclusions depended on model simulations. Anthropogenic warming estimated directly from the historical observations is more pronounced between 45°S and 50°N than at higher latitudes whereas the model-simulated trends have minimum values in the tropics and increase steadily from 30 to 70°N.
Citation: Lean, J. L., and D. H. Rind (2008), How natural and anthropogenic influences alter global and regional surface temperatures: 1889 to 2006, *Geophys. Res. Lett.*, *35*, L18701, doi:10.1029/2008GL034864.

1. Introduction

[2] Both natural and anthropogenic influences caused twentieth century climate change but their relative roles and regional impacts are still under debate. Especially controversial is the contribution of solar activity to global surface temperatures, which warmed at a rate of 0.74 K in the century from 1905 to 2005 [*Intergovernmental Panel on Climate Change* (*IPCC*), 2007]. An exhaustive model-based study concludes that increasing anthropogenic gas concentrations (GHGs and tropospheric aerosols) produced 0.3–0.5 K per century warming over the 1906–1996 period and are the dominant cause of global surface warming after 1976 [*Allen et al.*, 2006]. In contrast, recent empirical analyses suggest that solar variability accounts for as much as 69% of twentieth century warming, 25–35% of recent warming, globally [*Scafetta and West*, 2006, 2008], and produces a factor of two larger warming during the 11-year cycle than in prior studies [*Camp and Tung*, 2007]. Although less controversial, ENSO and volcanic impacts must also be properly quantified. The few tenths Kelvin warming during the November 1997 "super" El Niño elevated the global surface temperature beyond that in subsequent years, even as greenhouse gas concentrations increased, fueling debate about the reality of anthropogenic global warming.

[3] *IPCC* [2007] did not report geographical patterns of climate responses to individual natural and anthropogenic influences because of model uncertainties at smaller than continental scales and over time scales less than 50 years. Separating natural and anthropogenic surface temperature influences directly in the observed anomalies is difficult [*Santer et al.*, 2001]. Although ENSO variations occur primarily with periods of 2–4 years, and decadal variability is typically attributed to the solar cycle, volcanic cooling projects onto both the ENSO and solar signal, so that conclusions can differ depending on the analysis technique and epoch. One approach is to assume that surface temperatures respond linearly (at some lag) to the various influences, which are then separated by virtue of their different temporal structures using multiple regression analysis [e.g., *Santer et al.*, 2001; *Haigh*, 2003]. A different approach is to construct composite mean differences for individual events. By differencing years of solar maxima and minima in NCEP temperatures since 1959, *Camp and Tung* [2007] determined a solar cycle amplitude in global surface temperature of 0.2 K, a factor of two larger than obtained from multiple regression analysis of satellite data since 1979 [*Douglass and Clader*, 2002].

[4] Historical surface temperature records provide a significantly longer dataset than the NCEP reanalysis and space-based databases. Using the most recently available characterizations of ENSO, volcanic aerosols, solar irradiance and anthropogenic influences, we perform multiple linear regression analyses to decompose 118 years (11 complete solar cycles) of monthly mean surface temperature anomalies into four components. The decomposition is conducted for the global signals, and on a 5° × 5° latitude-longitude grid to determine the corresponding geographical patterns. We repeat the analysis for the NCEP and satellite epochs to establish that the approach is robust for datasets of different lengths, and we examine the evolution of decadal power in the natural influences to assess their projections onto each other as sources of error in prior results. Our results yield trends in the four individual global surface temperature components over the past 25, 50 and 100 years, augmenting the linear trends that IPCC reported in net global temperature for these same periods,

[1]Space Science Division, Naval Research Laboratory, Washington, D. C., USA.
[2]Goddard Institute for Space Studies, NASA, New York, New York, USA.

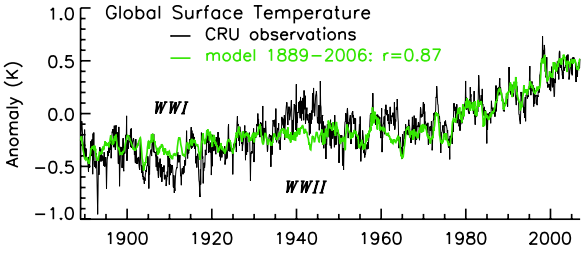

Figure 1. Compared with the CRU monthly mean global temperature time series (hadcrut3vcgl) is an empirical model obtained from multiple regression for the period from 1889 to 2006, inclusive. The value of r is the correlation coefficient for the global temperature observations and empirical model. Largest differences occur at the times of the two World Wars when observations were sparse.

and depicting the associated regional temperature trend patterns.

2. Datasets

[5] Shown in Figure 1 is the long-term instrumental record of monthly mean global (land plus ocean) surface temperature anomalies since 1889, constructed by the University of East Anglia Climatic Research Unit (CRU) [*Brohan et al.*, 2006]. Monthly fluctuations in ENSO, volcanic aerosols, solar irradiance and anthropogenic influences are shown in Figure 2. The multivariate ENSO index, a weighted average of the main ENSO features contained in sea-level pressure, surface wind, surface sea and air temperature, and cloudiness [*Wolter and Timlin*, 1998], extends from 1950 to 2006. It is augmented with an index derived from Japan Meteorologial Agency sea surface temperatures from 1868 [*Meyers et al.*, 1999]. Volcanic aerosols in the

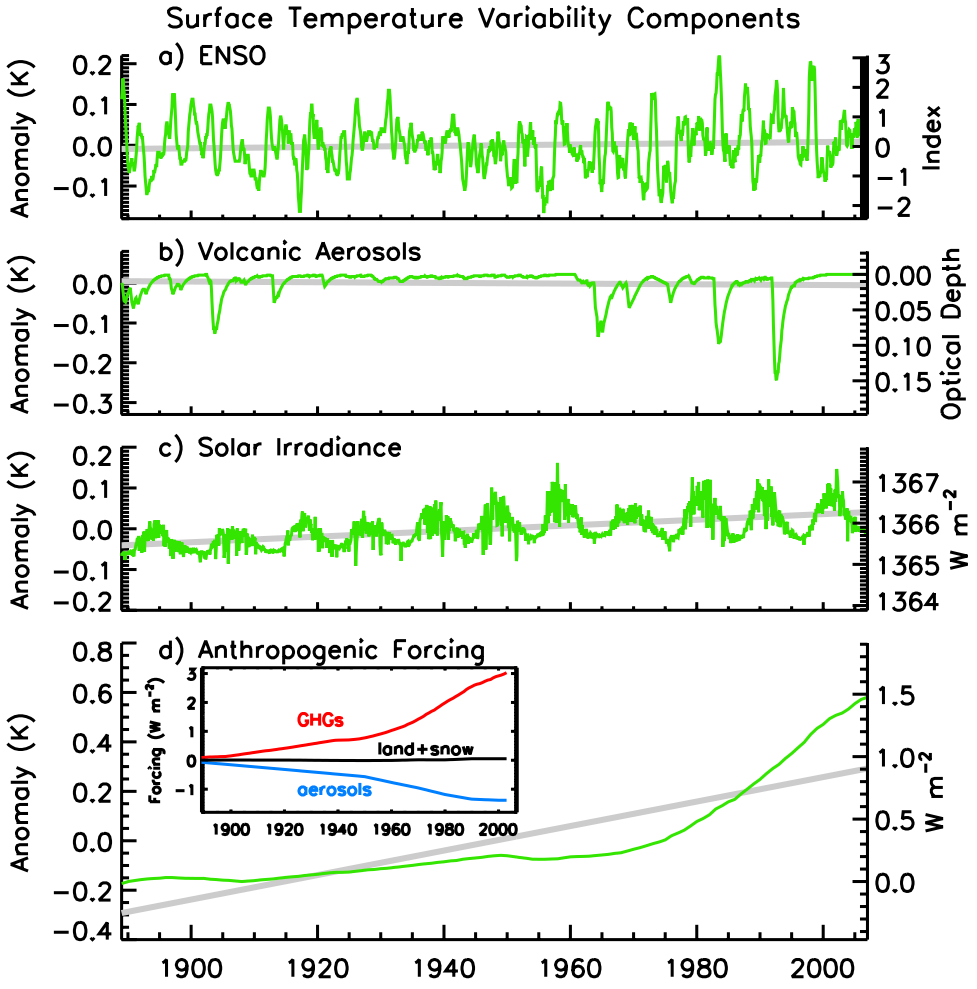

Figure 2. Reconstructions of the contributions to monthly mean global surface temperatures by individual natural and anthropogenic influences (at appropriate lags) are shown. The right hand ordinates give the native scales of each influence and the left hand ordinates give the corresponding temperature change determined from the multiple regression analysis. The grey lines are trends for the whole interval. The inset in Figure 2d shows the individual greenhouse gases, tropospheric aerosols and the land surface plus snow albedo components that combine to give the net anthropogenic forcing.

Table 1. Amplitudes of Global Temperature Trends Arising From Individual Natural and Anthropogenic Influences Determined As the Slopes of the Time Series in Figure 2 Over Different Epochs[a]

Period	ENSO	Volcanic Activity	Solar Activity	Anthropogenic Forcing	*IPCC* [2007] Temperature
1889–2006	0.0015 ± 0.0005	−0.0009 ± 0.0003	0.007 ± 0.001	0.050 ± 0.001	
100 yrs: 1905–2005	0.0028 ± 0.0006	−0.0029 ± 0.0004	0.007 ± 0.001	0.059 ± 0.001	0.074 ± 0.018
50 yrs: 1955–2005	0.015 ± 0.002	0.001 ± 0.001	0.002 ± 0.001	0.136 ± 0.003	0.128 ± 0.026
25 yrs: 1979–2005	−0.007 ± 0.005	0.018 ± 0.004	−0.004 ± 0.004	0.199 ± 0.005	0.177 ± 0.052

[a]The given uncertainties are the combined statistical uncertainties of the multiple regression and the fitted trend and do not include uncertainties in either the temperature observations or the forcings. *IPCC* [2007] net global temperature trends are included for comparison. Trends are in K per decade.

stratosphere are compiled by [*Sato et al.*, 1993] since 1850, updated from giss.nasa.gov to 1999 and extended to the present with zero values. The adopted solar forcing, consistent with *IPCC* [2007], is less than half that reported in prior IPCC assessments. Monthly irradiances since 1882 are estimated from competing effects of sunspots and faculae in observations made by space-based radiometers, extended into the past using solar flux transport simulations [*Wang et al.*, 2005]. The anthropogenic forcing is the net effect of eight different components, including greenhouse gases, landuse and snow albedo changes, and (admittedly uncertain) tropospheric aerosols [*Hansen et al.*, 2007] (inset, Figure 2d).

3. Analysis

[6] A reconstruction of monthly mean surface temperature anomalies, T_R, is determined from zero mean, unit variance time series of ENSO, E, volcanic aerosols, V, solar irradiance, S, and anthropogenic forcing, A, as $T_R(t) = c_0 + c_E E(t - \Delta t_E) + c_V V(t - \Delta t_V) + c_S S(t - \Delta t_S) + c_A A(t - \Delta t_A)$ where the lags (in months) are $\Delta t_E = 4$, $\Delta t_V = 6$, $\Delta t_S = 1$ and $\Delta t_A = 120$ (chosen to maximize the explained variance). The fitted coefficients, $c_0 \ldots$, their one sigma uncertainties, $\Delta c_0 \ldots$, and the correlation matrix are obtained by multiple linear regression.

[7] The combination of natural and anthropogenic components accounts for 76% of the variance in the CRU monthly data from 1889 to 2006. The fitted coefficients, all of which exceed their one sigma uncertainties (6% for ENSO, 10% for volcanic aerosols, 10% for solar irradiance and 2% for anthropogenic forcing), convert the time series in Figure 2 from their native units (on the right axis) to equivalent temperature anomalies (on the left axis). Table 1 lists the linear trends in the temperature anomalies attributable to each of the four individual influences over the entire period, and compares the trends in three intervals (past 25, 50 and 100 years) with IPCC's corresponding linear (net) global surface temperature trends.

[8] Geographical distributions of the responses are also estimated from multiple regression analysis. In this case, the $T_R(t)$ are determined for all monthly surface temperature anomalies in each 5° × 5° latitude-longitude grid. Fitted coefficients are determined for each pixel at the lag that maximizes the global responses (although a geographical dependence is expected for the lags). The spatial patterns shown in Figure 3 are the temperature changes in each pixel corresponding to 0.1 K global change, restricted to latitudes from 65°S to 70°N where the observations primarily exist [*Brohan et al.*, 2006]. Zonal means of the patterns are also shown in Figure 3, determined from the analysis over the entire epoch (1889–2006), and separately for the NCEP reanalysis period (1960–2006) and the satellite era (1980 to 2006). The qualitative similarity of the zonal trends derived from the three different epochs gives confidence that the patterns are robust.

4. Amplitudes and Patterns of Natural and Anthropogenic Influences

[9] ENSO and volcanic events are clearly identified as significant sources of variance in the historical surface temperature record. As a result of the 1997 "super" El Niño the globe warmed 0.23 ± 0.01 from June to November. The given uncertainty is the square root of the summed variance of the one-sigma uncertainties (from the multiple regression). The associated spatial pattern shows dominant ENSO impacts between ±30° with maximum impact at the equator. Northern hemisphere changes have distinct meridional asymmetry with strong North Pacific cooling and western continental US warming, consistent with known El Niño impacts of Alaskan warming and strengthened Aleutian low.

[10] The Pinatubo eruption produced global cooling of 0.25 ± 0.02 K from November 1991 to September 1992, primarily between 40°S and 70°N, and especially in the US and the North Atlantic Ocean. Slight warming in the northern Eurasian continent is consistent with known volcanic impacts of strengthened westerly winds and a more positive phase of the North Atlantic Oscillation [*Kodera*, 1994]. When deduced from multiple regression analysis of just the recent data (1980 to 2006) the estimated cooling is the same (0.25 K), and still smaller than the 0.35–0.45 K cooling that *Santer et al.* [2001] found over a similar time period. *Santer et al.* likely overestimated volcanic cooling by neglecting to account for the simultaneous solar and anthropogenic influences, since when the regression analysis is repeated using only ENSO and volcanic aerosols the volcanic cooling increases to 0.44 K.

[11] Solar activity is reliably detected in the global historical surface temperature record, for example, producing a peak monthly increase of 0.17 ± 0.01 K from April 1996 (solar minimum) to February 2002 (solar maximum). The 13-month running mean solar cycle change is 0.11 K at one month lag, consistent with the solar cycle signal found in lower troposphere satellite data since 1979 [*Douglass and Clader*, 2002]. The response is strongest at mid latitudes (near 40°) in both the Northern and Southern hemispheres, in the vicinity of the Ferrel cells, which interface the Hadley and Polar cells. The detectable amplitude and rapid response

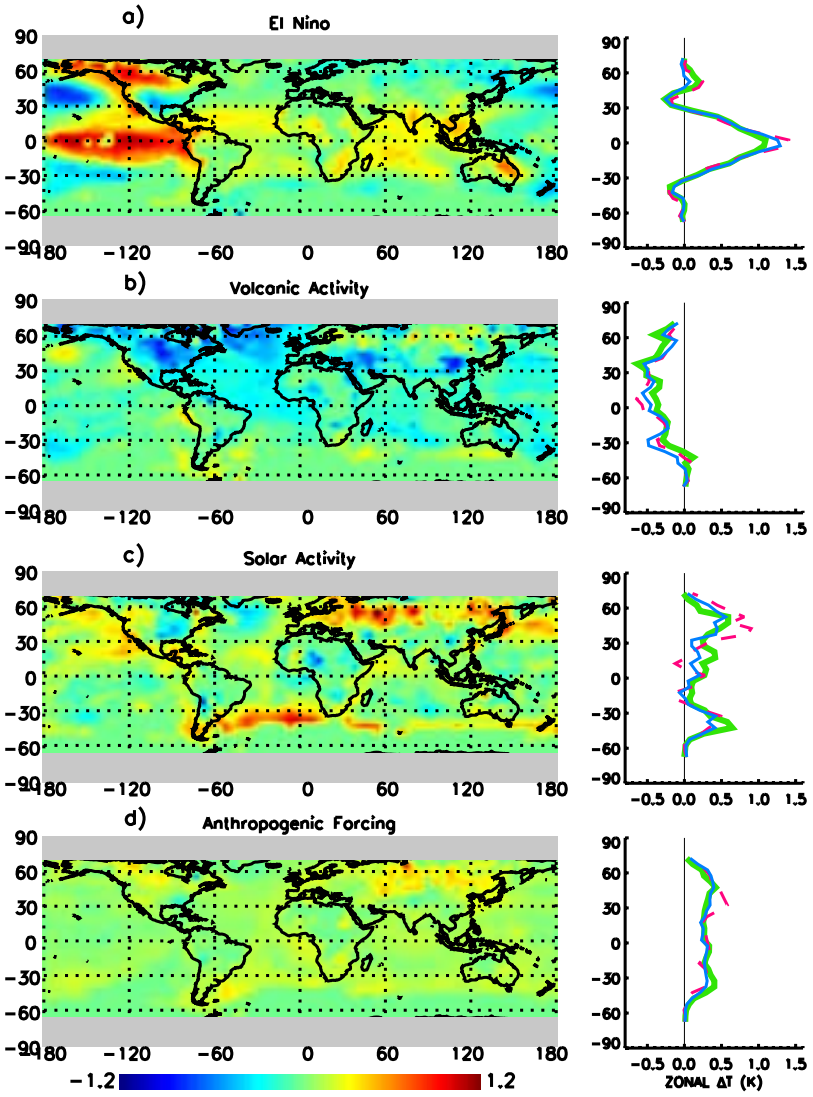

Figure 3. (left) Compared are geographical response patterns, each normalized to a 0.1 K global temperature change, due to ENSO, volcanic, solar and anthropogenic influences, derived from the monthly historical surface temperature records (1889–2006). (right) Also shown are zonal means of the geographical responses from the regression of data in three different epochs. The thick (green) curve is for the entire period from 1889 to 2006, the thin (blue) curve is for the NCEP period from 1960 to 2006 and the dashed (pink) curve is for the satellite era from 1980 to 2006.

of surface temperatures to decadal solar forcing is consistent with prior analyses of NCEP data, and suggests that the response involves the large-scale dynamical circulation of the atmosphere [*Haigh*, 2003; *van Loon et al.*, 2004].

[12] The 0.1 K (13-month mean) global solar cycle increase with modest warming at high latitudes (Figure 3) differs markedly from the 0.2 K solar cycle global increase dominated by significant high latitude warming that *Camp and Tung* [2007] derived by differencing solar cycle maximum and minimum epochs in the NCEP data. Their larger estimates of the solar cycle amplitude may be erroneous because of uncorrected volcanic cooling. Over the NCEP epoch decadal power in solar irradiance and volcanic aerosols is approximately in phase during two of the last five solar cycles. This is illustrated in Figure 4, which compares time variations in solar, volcanic and ENSO power in a band from 8.5 to 12.8 years, isolated in the

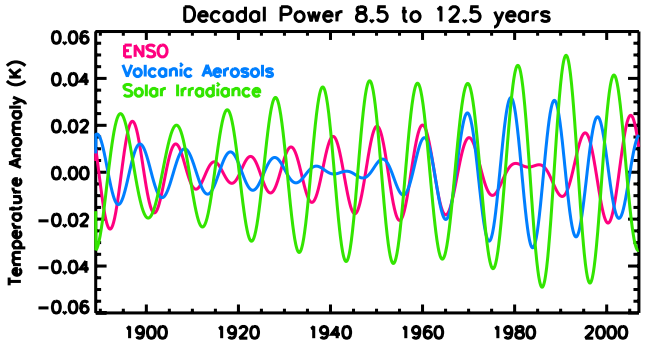

Figure 4. Shown are reconstructions of time series of the decadal signal in the ENSO, volcanic and solar time series in Figure 2, isolated by FFT filtering.

frequency domain by the FFT. Another explanation may be the significant contributions from high latitudes. The NCEP project assimilates available data onto model simulations so that the high latitude fields likely reflect modeled changes, since actual surface temperature observations are confined mainly to the region from 65°S to 70°N [*Brohan et al.*, 2006].

[13] Natural changes cannot account for the significant long-term warming in the historical global surface temperature anomalies. Linear trends in temperature attributed to ENSO, volcanic aerosols and solar irradiance over the past 118 years (depicted by the lines in Figure 2) are, respectively, 0.002, −0.001 and 0.007 K per decade. Only by associating the surface warming with anthropogenic forcing is it possible to reconstruct the observed temperature anomalies. The average anthropogenic-related warming is 0.05 K per decade from 1889 to 2006, which is in close agreement with that determined independently from *Allen et al.*'s [2006] synthesis of theoretical model studies. For the ninety years from 1906 to 1996, the average slope of the anthropogenic–related temperature change in Figure 3d is 0.045 K per decade whereas *Allen et al.* [2006] concluded that the rate is 0.03–0.05 K per decade for this same period. Solar-induced warming is almost an order of magnitude smaller. It contributes 10%, not 65% [*Scafetta and West*, 2006, 2008], of surface warming in the past 100 years and, if anything, a very slight overall cooling in the past 25 years (Table 1), not 20–30% of the warming.

[14] Contrary to recent assessments based on theoretical models [*IPCC*, 2007] the anthropogenic warming estimated directly from the historical observations is more pronounced between 45°S and 50°N than at higher latitudes (Figure 3d (right)). This is the approximate inverse of the model-simulated anthropogenic plus natural temperature trends in IPCC (Figure 9.6), which have minimum values in the tropics and increase steadily from 30 to 70°N. Furthermore, the empirically-derived zonal mean anthropogenic changes have approximate hemispheric symmetry whereas the mid-to-high latitude modeled changes are larger in the Northern hemisphere. Climate models may therefore lack – or incorrectly parameterize - fundamental processes by which surface temperatures respond to radiative forcings. Cloud responses, which affect the latitude response structure, are known to be uncertain in the models.

5. Summary

[15] Empirical models that combine natural and anthropogenic influences (at appropriate lags) capture 76% of the variance in the CRU monthly global surface temperature record, suggesting that much of the variability arises from processes that can be identified and their impact on the global surface temperature quantified by direct linear association with the observations.

[16] Natural influences produce as much as 0.2 K warming during major ENSO events, near 0.3 K cooling following large volcanic eruptions and 0.1 K warming near maxima of recent solar cycles. To properly quantify their amplitudes, the natural and anthropogenic changes must be accounted for simultaneously when analyzing the surface temperature anomalies, since neglecting the influence of one can overestimate the influence of another. For this reason, we suggest that estimated solar cycle changes of 0.2 K [*Camp and Tung*, 2007] and Pinatubo cooling of 0.4 K [*Santer et al.*, 2001] are too large.

[17] None of the natural processes can account for the overall warming trend in global surface temperatures. In the 100 years from 1905 to 2005, the temperature trends produce by all three natural influences are at least an order of magnitude smaller than the observed surface temperature trend reported by *IPCC* [2007]. According to this analysis, solar forcing contributed negligible long-term warming in the past 25 years and 10% of the warming in the past 100 years, not 69% as claimed by *Scafetta and West* [2008] (who assumed larger solar irradiance changes and enhanced climate response on longer time scales).

[18] In contrast with climate model simulations, the zonal surface temperature changes determined for natural (solar and volcanic) and anthropogenic influences from the historical surface temperature record do not increase rapidly from mid to high latitudes. Furthermore, since the temperature response to solar forcing occurs relatively rapidly (within months) with patterns that relate to existing tropospheric circulation patterns, the pathways likely involve dynamical motions not simply thermal processes that transfer heat to the deep ocean. With the goal of using the geographical patterns to quantitatively constrain simulated climate change, detailed comparisons with the GISS middle atmosphere GCM are underway. So too is an assessment of the seasonal dependences of the responses to natural and anthropogenic influences reported here using all months (i.e., without seasonal discrimination), and of their upward propagation in the atmosphere.

[19] **Acknowledgments.** NASA LWS and SORCE funded this work. Data were obtained from http://www.cru.uea.ac.uk/, http://www.cdc.noaa.gov/ENSO/enso.mei_index.html and http://www.giss.nasa.gov/. Appreciated are efforts of the many scientists who maintain the various datasets and make them readily available.

References

Allen, M. R., et al. (2006), Quantifying anthropogenic influence on recent near-surface temperature change, *Surv. Geophys.*, *27*, 491–544, doi:10.1007/s10712-006-9011-6.

Brohan, P., J. J. Kennedy, I. Harris, S. F. B. Tett, and P. D. Jones (2006), Uncertainty estimates in regional and global observed temperature changes: A new dataset from 1850, *J. Geophys. Res.*, *111*, D12106, doi:10.1029/2005JD006548.

Camp, C. D., and K. K. Tung (2007), Surface warming by the solar cycle as revealed by the composite mean difference projection, *Geophys. Res. Lett.*, *34*, L14703, doi:10.1029/2007GL030207.

Douglass, D. H., and B. D. Clader (2002), Climate sensitivity of the Earth to solar irradiance, *Geophys. Res. Lett.*, *29*(16), 1786, doi:10.1029/2002GL015345.

Haigh, J. D. (2003), The effects of solar variability on the Earth's climate, *Philos. Trans. R. Soc. London Ser. A*, *361*, 95–111.

Hansen, J., et al. (2007), Climate simulations for 1880–2003 with GISS modelE, *Clim. Dyn.*, *29*, 661–696, doi:10.1007/s00382-007-0255-8.

Intergovernmental Panel on Climate Change (2007), Climate Change 2007: The Physical Science Basis, Contribution of Working Group I to the Fourth Assessment Report of the Intergovernmental Panel on Climate Change, edited by S. Solomon et al., Cambridge Univ. Press, Cambridge, U. K.

Kodera, K. (1994), Influence of volcanic eruptions on the troposphere through stratospheric dynamical processes in the Northern Hemisphere winter, *J. Geophys. Res.*, *99*, 1273–1282.

Meyers, S. D., J. J. O'Brien, and E. Thelin (1999), Reconstruction of monthly SST in the tropical Pacific Ocean during 1868–1993 using adaptive climate basis functions, *Mon. Weather Rev.*, *127*, 1599–1612.

Santer, B. D., T. M. L. Wigley, C. Doutriaux, J. S. Boyle, J. E. Hansen, P. D. Jones, G. A. Meehl, E. Roeckner, S. Sengupta, and K. E. Taylor (2001), Accounting for the effects of volcanoes and ENSO in comparisons of

modeled and observed temperature trends, *J. Geophys. Res.*, *106*, 28,033–28,059.

Sato, M., J. E. Hansen, M. P. McCormick, and J. B. Pollack (1993), Stratospheric aerosol optical depths, 1850–1990, *J. Geophys. Res.*, *98*, 22,987–22,994.

Scafetta, N., and B. J. West (2006), Phenomenological solar contribution to the 1900–2000 global surface warming, *Geophys. Res. Lett.*, *33*, L05708, doi:10.1029/2005GL025539.

Scafetta, N., and B. J. West (2008), Is climate sensitive to solar variability?, *Phys. Today*, *3*, 50–51, March.

van Loon, H., G. A. Meehl, and J. M. Arblaster (2004), A decadal solar effect in the tropics in July–August, *J. Atmos. Sol. Terr. Phys.*, *66*, 1767–1778.

Wang, Y.-M., J. L. Lean, and N. R. Sheeley Jr. (2005), Modeling the Sun's magnetic field and irradiance since 1713, *Astrophys. J.*, *625*, 522–538.

Wolter, K., and M. S. Timlin (1998), Measuring the strength of ENSO: How does 1997/98 rank?, *Weather*, *53*, 315–324.

J. L. Lean, Space Science Division, Naval Research Laboratory, Washington, DC 20375, USA. (judith.lean@nrl.navy.mil)

D. H. Rind, Goddard Institute for Space Studies, NASA, New York, NY 10025, USA.